

Bearing-Only Localization Using Geometrically Constrained Optimization

Adrian N. Bishop, *Student Member, IEEE*, Brian D.O. Anderson, *Life Fellow, IEEE*, Barış Fidan, *Member, IEEE*, Pubudu N. Pathirana and Guoqiang Mao, *Member, IEEE*

Abstract—In this paper we examine the geometric relations between various measured parameters and their corresponding errors in angle-measurement based emitter localization scenarios. We derive a geometric constraint formulating the relationship among the measurement errors in such a scenario. Using this constraint, we formulate the localization task as a constrained optimization problem that can be performed on the measurements in order to provide the optimal values such that the solution is consistent with the underlying geometry. We illustrate and confirm the advantages of our approach through simulation.

Index Terms—Angle Measurements, Bearings, Geometric Constraints, Localization, Optimization, Tracking.

I. INTRODUCTION

BEARING sensors measure the direction to the target with respect to a global or local direction [1], [2], [3], [4] and often permit passive localization by exploiting the characteristics of an emitter’s signal rather than requiring active signal generation. The problem of angle-based localization and tracking was of considerable interest during World War II [5], [6] but has some roots dating back even further [7]. The majority of the approaches examine the problem from a statistical estimation point of view. Assumptions on noise distributions and the resulting optimization algorithms make little attempt to directly exploit the underlying geometrical properties of the required localization solution.

Stansfield in [5] provided a closed-form small error approximation of the maximum likelihood estimator in 1947. Stansfield assumed that the residual can be replaced with the sine of the residual and that the range from each sensor to the target may be approximately known. Under these assumptions, a closed-form solution is possible and given in [5] and rigorously analysed in [8]. It is shown in [8] that the Stansfield estimator is asymptotically biased.

A linearized least squares approach to bearings-based localization was given in [9]. This method attempts to approximate the maximum likelihood estimator and may result in large localization errors when the measurement noise is large or the

geometry is adversely suited to accurate localization. Another approach to maximum likelihood localization using iteration was given in [10]. Note that under normal density assumptions, the maximum likelihood cost function is simply a weighted nonlinear least squares cost function. Closed-form solutions do not exist for finding the global minimum of such cost functions and the linearized and iterative algorithms typically require an initial estimate of the target location [10], [9], [8], [11]. In [8] the traditional maximum likelihood formulation (abbreviated as TML henceforth) is examined in detail including a bias and variance analysis. A separate analysis is also conducted in [11] and the reader is referred to these two papers [11], [8] for further information on the TML approach.

In this paper we focus particularly on the localization problem for a single stationary target. Other bearing-only localization and tracking problems exist and complement the work of this paper. The *multiple target* localization problem can be broken down into multiple single target localization problems if the measurement origins are known (i.e. if the measurements can be uniquely assigned to individual targets). If the measurement origins are unknown then the so-called *data-association* problem needs to be addressed. There exists a number of papers in the literature that address this problem, e.g. see [12], [13], [14], [15], [16], [17]. Some of these papers also take into account so-called missing measurements and false alarms caused by clutter and electronic counter-measures. *Mobile target tracking* with bearing measurements has been addressed in a number of papers and various problems exist, e.g. see [18], [11], [19], [20], [21] and the references therein.

The principal and immediate objective of this paper is to explicitly derive and examine functional relationships (which depend on the measurements and are rooted in geometry) between the measurement errors in a passive surveillance scenario. We seek to form a constraint that can be used in a constrained optimization process where the aim of the process is to minimize the location estimation error for a single target. Indeed the errors may be estimated such that the final solution satisfies the proposed constraint and hence is consistent with the geometry. The ultimate goal is to derive a maximum likelihood localization algorithm that is *robust against initialization errors and that can converge in the presence of adverse localization geometries*.

Constraint-based optimization in localization systems may have first been introduced within the computer vision community [22], [23], [24]. In [22] the epipolar constraint is used to derive an optimal localization algorithm for stereo vision systems. The epipolar constraint relates a point image

A.N. Bishop and P.N. Pathirana are with the School of Engineering and Information Technology, Deakin University. B.D.O. Anderson and B. Fidan are with the Australian National University and National ICT Australia. G. Mao is with the University of Sydney and National ICT Australia.

The work of A.N. Bishop and P.N. Pathirana was supported by the Australian Research Council. The work of B.D.O. Anderson, B. Fidan and G. Mao was supported by National ICT Australia. National ICT Australia is funded by the Australian Government’s Department of Communications, Information Technology and the Arts and the Australian Research Council through the Backing Australia’s Ability Initiative and the ICT Centre of Excellence Program.

in one camera view to the corresponding point image in the second camera view based on epipolar geometry. This relationship then acts as a constraint in the presence of noisy measurements. The vision-based localization problem is extended in [24] for three cameras. Geometric constraints have also been examined for distance-based localization in [25] where a convex quadratic constraint is given on the squared distance measurement errors. One of the contributions of this paper is the development of such a geometric constraint for bearing-based localization.

We illustrate our algorithm's relationship to the traditional maximum likelihood algorithm (TML) [11], [8]. The constrained optimization algorithm derived in this paper will be statistically optimal in the maximum likelihood sense but will not require an initial estimate of the target location. It is this initial target location estimate that often results in the TML algorithm diverging in adverse localization geometries, i.e. the TML initialization is geometry-dependent [10], [8]. Our algorithm can be initialized more naturally in the light of known measurement error statistics and is geometry-invariant. This is by no means a trivial advantage and is a major contribution of this paper since it addresses the practical problems associated with the traditionally formulated maximum likelihood algorithm.

The remainder of this paper is organized as follows. In Section II we formulate the problem and derive a functional relationship between the bearing errors in \mathbb{R}^2 and \mathbb{R}^3 . Section III outlines the inconsistency problem associated with the over-determined system of measurement equations from a geometric perspective and outlines the solution to the problem conceptually. Section IV discusses the constrained optimization algorithm used to find a consistent solution to the problem and in Section 5 we illustrate the proposed concepts through simulation. In Section V we also discuss our technique's relationship to the traditional least squares approach. In Section VI we give our concluding remarks.

II. ANGLE CONSTRAINTS FOR PASSIVE SURVEILLANCE

A. Problems in \mathbb{R}^2

Consider the problem of localizing an emitter in \mathbb{R}^2 using measurements from two bearing sensors. The two bearing measurement equations will lead to a solution for the two unknowns (i.e. the x and y coordinates of the target), and the solution is unique (though not in general error free) even in the presence of noisy measurements. With three or more bearing sensors in \mathbb{R}^2 we obtain an overdetermined system of equations with respect to the unknown target coordinates. In a noiseless environment the overdetermined system will have a unique solution. In a noisy environment, the overdetermined system of equations will generally not have any solution. We consider the problem of formulating a relationship between the measurement errors such that the measurement equations permit a consistent solution for the unknown target location.

Each sensor measures the bearing to the target relative to a global direction (e.g. North). Call those bearing estimates $\hat{\phi}_{1T}$, $\hat{\phi}_{2T}$ and $\hat{\phi}_{3T}$. These have errors e_i such that the true bearings ϕ_{iT} obey $\hat{\phi}_{iT} = \phi_{iT} + e_i$. Also, we have available exactly the

inter-sensor bearings ϕ_{12} and ϕ_{13} etc. We define the bearings such that $\hat{\phi}_{iT}, \phi_{ij} \in [0, 2\pi)$. The unit of angle is radians and we further assume that all calculations are performed in radians (this distinction will be important when it comes to approximating functions). The unit of degrees will only sparingly be used for illustrative convenience. The following will be adopted as a Standing Assumption for the whole paper:

Assumption 1: No sensors are co-located with and no two sensors are collinear with a single target, i.e. $\phi_{iT} \neq \phi_{ij} \forall i, j \in \{1, 2, 3\}$ and $i \neq j$.

Note that the assumption does not necessarily imply that $\hat{\phi}_{iT} \neq \phi_{ij}$.

Let us define an angle $\theta_{ijT} \equiv (\phi_{iT} - \phi_{ij})(\text{mod } 2\pi)$ and restrict the interval such that $\theta_{ijT} \in (-\pi, \pi]$. Geometrically we can interpret θ_{ijT} to be the angle obtained by rotating a ray counter-clockwise from the line segment connecting sensors i and j to the line segment connecting the sensor i and the target T . Therefore, it is clear that $\theta_{ijT} = -\theta_{iTj}$ and due to the notion of orientation inherent in the definition of θ_{ijT} it follows that θ_{ijT} and θ_{jiT} will be of opposite sign. The error in the measured angle $\hat{\theta}_{ijT} = \theta_{ijT} + e_i$ obeys $e_i \in (-\pi, \pi]$ and coincides with the typical notion of error.

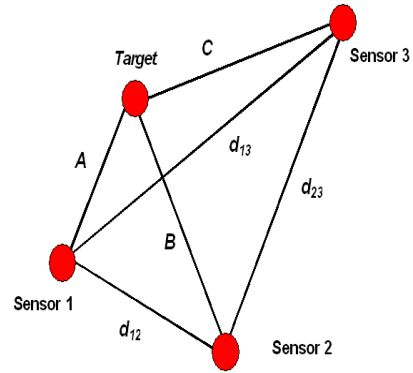


Fig. 1. Sensors-Target System in \mathbb{R}^2

Generally for any system of three sensors and a single target, Figure 1, we can determine six angles that are related to their measured counterparts via

$$\hat{\theta}_{ijT} = \theta_{ijT} + e_i \quad (1)$$

and $i, j \in \{1, 2, 3\}$ with $i \neq j$. Note that for any j , $\hat{\theta}_{ijT}$ (being an angle measured by sensor i) involves only the error e_i .

Theorem 1: Consider an arrangement of three sensors and a target all located in the plane, e.g. as shown in Figure 1 and assume Assumption 1 holds. Suppose that we have available the associated six quantities as indicated in (1) and as previously defined. Then in terms of the known quantities $\hat{\theta}_{ijT}$, the unknown measurement errors satisfy the following trigonometric constraint

$$\sin(\hat{\theta}_{12T} - e_1) \sin(\hat{\theta}_{23T} - e_2) \sin(\hat{\theta}_{31T} - e_3) + \sin(\hat{\theta}_{21T} - e_2) \sin(\hat{\theta}_{32T} - e_3) \sin(\hat{\theta}_{13T} - e_1) = 0 \quad (2)$$

where $e_i, \forall i \in \{1, 2, 3\}$ are errors.

Proof: Recall that the definitions of θ_{ijT} and θ_{jiT} imply that the two quantities are of opposite sign. Then from the

well-known law of sines, a system of equations can be given as follows

$$A \sin(\theta_{12T}) + B \sin(\theta_{21T}) = 0 \quad (3)$$

$$B \sin(\theta_{23T}) + C \sin(\theta_{32T}) = 0 \quad (4)$$

$$A \sin(\theta_{13T}) + C \sin(\theta_{31T}) = 0 \quad (5)$$

Eliminating A , B and C leads to

$$\begin{aligned} & \sin(\theta_{12T}) \sin(\theta_{23T}) \sin(\theta_{31T}) + \\ & \sin(\theta_{21T}) \sin(\theta_{32T}) \sin(\theta_{13T}) = 0 \end{aligned} \quad (6)$$

Now (6) is a relationship between the angles of the triangle system. By adding the corresponding error term to both sides of each equation in (1) and substituting into (6) we obtain the constraint equation (2) on the measurement errors. ■

Remark 1: The condition (2) given on the measurement errors in Theorem 1 is not useful when the sensors are collinear with each other (but not with the target). When this occurs $\sin(\hat{\theta}_{ijT} + e_i) = -\sin(\hat{\theta}_{ikT} + e_i)$ for $i, j, k \in \{1, 2, 3\}$ and $i \neq j \neq k$ and for any value of e_i . Accordingly, for fixed measurements $\hat{\theta}_{ijT}$, the formula (2) will be satisfied with all values of e_i . Thus (2) fails to provide any constraint on the errors in this particular scenario.

For completeness, we provide a general constraint equation that is useful in all geometries including those involving three collinear sensors but that includes some inter-sensor distances. The constraint (2) has the advantage of involving only the measured angle values as parameters.

Theorem 2: Consider three bearing sensors satisfying Assumption 1. Assume that for each sensor pair i, j , the distance d_{ij} between i and j is known. Then in terms of the known quantities $\hat{\theta}_{ijT}$ and d_{ij} , the unknown measurement errors satisfy the following trigonometric constraint

$$\begin{aligned} & d_{12} \sin(\hat{\theta}_{12T} - e_1) \sin(\hat{\theta}_{23T} - e_2 + \hat{\theta}_{32T} - e_3) - \\ & d_{23} \sin(\hat{\theta}_{32T} - e_3) \sin(\hat{\theta}_{12T} - e_1 + \hat{\theta}_{21T} - e_2) = 0 \end{aligned} \quad (7)$$

where $e_i, \forall i \in \{1, 2, 3\}$ are errors.

Proof: Referring to Figure 1 and the system (1), a system of equations can be given as follows

$$B = \frac{d_{12} \sin(\theta_{12T})}{\sin(\theta_{12T} + \theta_{21T})} \quad (8)$$

$$B = \frac{d_{23} \sin(\theta_{32T})}{\sin(\theta_{23T} + \theta_{32T})} \quad (9)$$

This clearly leads directly to

$$\begin{aligned} & d_{12} \sin(\theta_{12T}) \sin(\theta_{23T} + \theta_{32T}) - \\ & d_{23} \sin(\theta_{32T}) \sin(\theta_{12T} + \theta_{21T}) = 0 \end{aligned} \quad (10)$$

Therefore, (10) is a trigonometric relationship between the angles of the triangle system. By adding the corresponding error term to both sides of each equation in (1) and substituting into (10) we obtain the constraint equation (7). ■

If the problem involves $k > 3$ measurements then we can derive $k - 2$ independent constraints of the form

$$c_{i-2}(e_1, e_2, e_i) = 0, \quad \forall i \in \{3, 4, \dots, k\} \quad (11)$$

These equations are obtained by considering the relations for the angles involving the target and a sensor triangle including sensors 1, 2 and $i, \forall i \in \{3, 4, \dots, k\}$.

B. Problems in \mathbb{R}^3

In \mathbb{R}^3 , it will generally be the case that two rays emanating from two sensors will not have a single intersection in the presence of noisy measurements. Consider the scenario depicted in Figure 2 involving sensor 1 and sensor 2. The plane including the two sensors and the point A is the horizontal plane (or (x, y) -plane) and AT is normal to that plane.

Remark 2: The choice of coordinate basis is determined first by locating sensor 1 at the origin, secondly by locating sensor 2 on the positive x -axis, and thirdly by defining the direction of the horizontal, or equivalently, choosing orientations for the y and z axis, which are only determined up to a rotation by sensors 1 and 2.

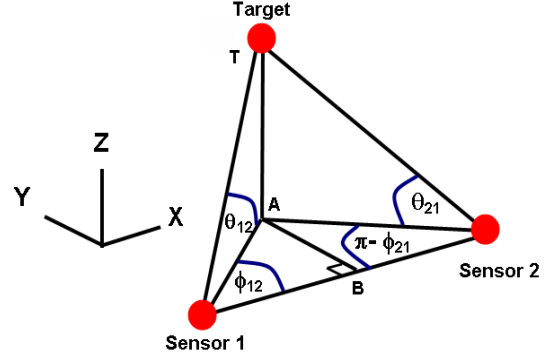


Fig. 2. Sensor configuration in \mathbb{R}^3 . The point A lies in the (x, y) -plane and AT is perpendicular to the (x, y) -plane.

The measurements taken via the passive localization system in \mathbb{R}^3 can be given as

$$\begin{aligned} \hat{\theta}_{ij} &= \theta_{ij} + e_{\theta_{ij}} \\ \hat{\phi}_{ij} &= \phi_{ij} + e_{\phi_{ij}}, \quad i, j \in \{1, 2\}, i \neq j \end{aligned}$$

where θ_{ij} and ϕ_{ij} are the true elevation and azimuth angles with respect to the origin of the coordinate system defined by sensors i and j and taken at the i^{th} sensor. The *hatted* versions are the noise corrupted measurements and $e_{\theta_{ij}}$ and $e_{\phi_{ij}}$ are the respective error values.

Theorem 3: Assume the choice of coordinate system agrees with Remark 2 and the depiction in Figure 2. Then in terms of the known quantities $\hat{\theta}_{ij}$ and $\hat{\phi}_{ij}$ for $i, j \in \{1, 2\}$ the unknown measurement errors satisfy the following trigonometric constraint

$$\begin{aligned} & \cot(\hat{\theta}_{12} - e_{\theta_{12}}) \sin(\hat{\phi}_{12} - e_{\phi_{12}}) - \\ & \cot(\hat{\theta}_{21} - e_{\theta_{21}}) \sin(\hat{\phi}_{21} - e_{\phi_{21}}) = 0 \end{aligned} \quad (12)$$

where $e_{\theta_{ij}}$ and $e_{\phi_{ij}}$ are the elevation and azimuth bearing errors respectively.

Proof: Referring to Figure 2, a system of equations can be given as follows

$$\begin{aligned} AB &= AS_1 \sin(\phi_{12}) = AT \cot(\theta_{12}) \sin(\phi_{12}) \\ AB &= AS_2 \sin(\pi - \phi_{21}) = AT \cot(\theta_{21}) \sin(\phi_{21}) \end{aligned} \quad (13)$$

where AS_i is the distance of the line segment connecting point A and sensor i . Eliminating the distances AB , AS_k and AT

from the system gives

$$\cot(\theta_{12}) \sin(\phi_{12}) - \cot(\theta_{21}) \sin(\phi_{21}) = 0 \quad (14)$$

Therefore, (14) is a trigonometric relationship between the bearing measurements in a 3-dimensional localization problem. By adding the corresponding error term to both sides of each equation in (12) and substituting into (14) we obtain the constraint equation (12). ■

If the problem involves $k > 2$ sensors then we have $k - 1$ independent constraints by creating constraints of the form

$$c_{i-1}(e_{\theta_{1i}}, e_{\phi_{1i}}, e_{\theta_{i1}}, e_{\phi_{i1}}) = 0, \quad \forall i \in \{2, 3, \dots, k\} \quad (15)$$

These equations are obtained by considering the relations for the angles involving the target and sensors 1 and i , $\forall i \in \{2, 3, \dots, k\}$. Note that we may also require each pair of sensors 1 and i , for $i = 2, 3, \dots, k$ to be arranged on their own coordinate system defined by sensors 1 and i and an associated choice of horizontal plane (specific to these two sensors); sensor 1 can remain at the origin and sensor i on a local positive x -axis specific to the two sensors. Thus the coordinate system for sensors 1 and $i > 2$ is obtained from that for sensors 1 and 2 by rotation but not translation.

III. GEOMETRIC INTERPRETATIONS

In this section we consider the underlying geometric interpretations of the problems considered in this paper and explore simple alternative approaches to localization. We look at the methods that are required to find solutions to the overdetermined localization problems and hence further motivate the work explored in this paper.

A. Geometry in \mathbb{R}^2

If we attempt to localize a single target in \mathbb{R}^2 using three bearing measurements from three generically placed sensors we can obtain an overdetermined system of equations in the target location (i.e. the x and y coordinates). In an ideal case there will be a unique solution to this overdetermined system of equations. In practice, i.e. in the presence of noise, it will generally be the case that there will be no (exact) solution to the system. One approach that may be followed in the presence of noisy measurements is to do pair-wise localization from the three pairs of well-defined systems. The result is depicted in Figure 3.

We can estimate the mean position of the three estimates as follows

$$\begin{aligned} x_{mean} &= (x_{1:2} + x_{1:3} + x_{2:3})/3 \\ y_{mean} &= (y_{1:2} + y_{1:3} + y_{2:3})/3 \end{aligned} \quad (16)$$

where $x_{i:j}$ and $y_{i:j}$ are the x and y estimates found by solving the well-defined system of measurement equations from sensors i and j . This is an ad-hoc way of localizing, and generically the errors associated with this estimate will fail to satisfy (2) or (7). In [26] the bias and variance of such an estimator is derived for the case of two bearing sensors and a single target and the extension to multiple bearing sensors is straightforward. The pseudo-linear estimator [11]

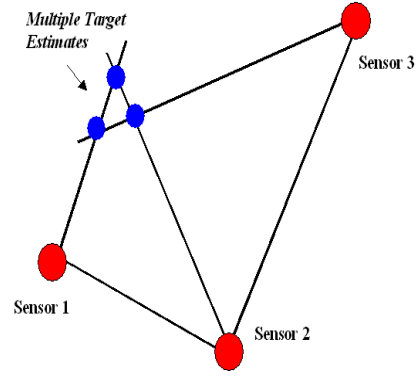


Fig. 3. Inconsistent system in \mathbb{R}^2

is an alternative closed-form approach that is similar to the given averaging approach in principle. Given the existence of the constraint on the errors in the system, we should seek to estimate a position for which the associated errors are consistent with (2) and (7). We will enforce this constraint by estimating the errors through a constrained optimization process.

B. Geometry in \mathbb{R}^3

In \mathbb{R}^3 the two virtual rays emanating from the two sensors will generally have no intersection in the presence of noise corrupted measurements. One approach to find a location solution that appears to not have been considered in the literature is to simply solve the triples of well-defined systems of equations and then take the average value of these estimates as we now describe. Considering two sensors and the resulting four measurement equations then we know that we cannot find an exact solution to the overdetermined system with noisy data, other than for nongeneric values of the noise. However, from the four equations we have four well-defined systems of three equations. We can solve all of these systems of equations for the target position and then find the average target position. That is, we find

$$\begin{aligned} x_{mean} &= (x_{\theta_{12}:\phi_{12}:\theta_{21}} + x_{\theta_{12}:\phi_{12}:\phi_{21}} + \\ &\quad x_{\theta_{12}:\theta_{21}:\phi_{21}} + x_{\phi_{12}:\theta_{21}:\phi_{21}})/4 \\ y_{mean} &= (y_{\theta_{12}:\phi_{12}:\theta_{21}} + y_{\theta_{12}:\phi_{12}:\phi_{21}} + \\ &\quad y_{\theta_{12}:\theta_{21}:\phi_{21}} + y_{\phi_{12}:\theta_{21}:\phi_{21}})/4 \\ z_{mean} &= (z_{\theta_{12}:\phi_{12}:\theta_{21}} + z_{\theta_{12}:\phi_{12}:\phi_{21}} + \\ &\quad z_{\theta_{12}:\theta_{21}:\phi_{21}} + z_{\phi_{12}:\theta_{21}:\phi_{21}})/4 \end{aligned} \quad (17)$$

where $x_{\theta_{12}:\phi_{12}:\theta_{21}}$ is the target's x coordinate determined using the well-determined system of measurements given by θ_{12} , ϕ_{12} , and θ_{21} , and so on for the other terms in (17).

An alternative method to find an estimate from the noisy information defining the two rays emanating from two sensors in \mathbb{R}^3 is to find the unique line that intersects both rays perpendicularly, and choose the midpoint between the two intersection points. Such a line always exists in \mathbb{R}^3 . However, this method of localization is practically difficult to implement and may permit large large localization errors [22]; its will not be covered further in this paper. The pseudo-linear estimator

(or linear least squares approach) as discussed for \mathbb{R}^2 can be extended to the \mathbb{R}^3 case [27] and is again similar to the given averaging approach in principle.

Given the error constraint for the \mathbb{R}^3 problem (12) we will attempt to estimate the errors that ensure a location solution that is consistent with the underlying geometry. The approach we take to do this is based on constrained optimization theory. This approach forces an underlying geometrical property of the system while at the same time attempts to minimize the effect of the errors.

C. Traditional Maximum Likelihood

In both \mathbb{R}^2 and \mathbb{R}^3 the traditionally formulated maximum likelihood (TML) algorithm (e.g. see [10], [9], [8], [11]) permits a consistent target location solution at the maximum of the likelihood cost function. Under the usual Gaussian error assumptions this target location is found by minimizing a nonconvex and nonlinear least squares cost function. To find the minimum requires a numerical optimization algorithm and an initial target location estimate that may play a critical role in the optimization convergence and in finding the global minimum. The initial target estimate may be derived from the previously described closed-form averaging location estimates. We shall show in the subsequent simulations that the TML algorithm may diverge in the presence of adverse localization geometries due to poor initialization. Again the reader is referred to [8], [11] for more details on the TML algorithms. In the simulations given subsequently we implement the TML algorithm with a Gauss-Newton algorithm as discussed in [8].

IV. THE CONSTRAINED OPTIMIZATION APPROACH

The constraints on the measurement errors discussed in the previous sections can be used in finding an optimal solution to the localization problem after formulating the problem as a constrained optimization problem [28], [29]. In this paper we will illustrate the proposed concept via a constrained least squares optimization problem. In \mathbb{R}^2 , we consider the following objective function

$$f(e_1, e_2, e_3, \dots) = e_1^2 + e_2^2 + e_3^2 + \dots \quad (18)$$

In the \mathbb{R}^2 case, we want to minimize the cost function in (18) subject to the system of constraints $c_{i-2}(e_1, e_2, e_i) = 0$ for $i \in \{3, \dots\}$ where each $c_{i-2}(e_1, e_2, e_i)$ is in the form of equation (2) or (7). In \mathbb{R}^3 , we consider the following objective function

$$f(e_{\theta 12}, e_{\phi 12}, e_{\theta 21}, e_{\phi 21}, \dots) = e_{\theta 12}^2 + e_{\phi 12}^2 + e_{\theta 21}^2 + e_{\phi 21}^2 + \dots \quad (19)$$

In the \mathbb{R}^3 case, we want to minimize (19) subject to the system of constraints $c_{i-1}(e_{\theta 1i}, e_{\phi 1i}, e_{\theta i1}, e_{\phi i1}) = 0$ for $i \in \{2, \dots\}$ where each $c_{i-1}(e_{\theta 1i}, e_{\phi 1i}, e_{\theta i1}, e_{\phi i1}) = 0$ is in the form of equation (12).

The formulas (18) and (19) can be thought of as coming up with a maximum likelihood estimation of the errors, given that they satisfy the particular constraints and that the errors (viewed as random variables) are mutually independent and

have the same variances. If the variances are different and/or the errors are correlated, then given an *a priori* estimate of the variances or covariance matrix we can modify the formulas (18) and (19) to the required form $f = \mathbf{e}^T \mathbf{\Sigma} \mathbf{e}$ where \mathbf{e} is an appropriately constructed error vector and $\mathbf{\Sigma}$ is the corresponding covariance matrix associated with \mathbf{e} .

Remark 3: It is important to note that the algorithm we outline is adaptable to other cost functions. The least squares approach is only equivalent to the maximum likelihood approach under the usual Gaussian assumptions. There may be cases when an L^1 norm or a different cost function is better suited to the problem. For example, the L^1 norm is generally considered more robust against large outliers.

Due to the nonlinearity of the constraints we employ the Sequential Quadratic Programming (SQP) technique [28], [30] to solve the required optimization problem. Sequential Quadratic Programming mimics Newton's method for unconstrained optimization. Consider the following general nonlinear programming problem

$$\begin{aligned} \text{argmin} \quad & f(\mathbf{x}) \\ \text{s.t.} \quad & c(\mathbf{x}) = 0 \end{aligned} \quad (20)$$

where $f(\mathbf{x})$ is a nonlinear objective function and $c(\mathbf{x})$ is a sufficiently differentiable nonlinear constraint function. The Lagrangian function associated with the problem (20) is

$$\mathcal{L} = f(\mathbf{x}) + \lambda^T c(\mathbf{x}) \quad (21)$$

At the i^{th} iteration, let \mathbf{x}_i be an estimate of the optimal solution \mathbf{x}^* and let λ_i be an estimate of the associated optimal Lagrange multipliers λ^* . Therefore, we can approximate the problem (20) by the following quadratic programming problem at the i^{th} iteration

$$\begin{aligned} \text{argmin} \quad & \frac{1}{2} \mathbf{p}^T \mathbf{H}_i \mathbf{p} + \nabla f(\mathbf{x}_i)^T \mathbf{p} \\ \text{s.t.} \quad & \nabla c(\mathbf{x}_i)^T \mathbf{p} + c(\mathbf{x}_i) = 0 \end{aligned} \quad (22)$$

where \mathbf{H} is the Hessian of the Lagrangian (21). A solution \mathbf{p}_i solves the problem (22) if and only if the standard Karush-Kuhn-Tucker (KKT) equations are satisfied with a given μ_i . That is,

$$\begin{bmatrix} \mathbf{H}_i & -\nabla c(\mathbf{x}_i)^T \\ -\nabla c(\mathbf{x}_i) & 0 \end{bmatrix} \begin{bmatrix} \mathbf{p}_i \\ \mu_i \end{bmatrix} = \begin{bmatrix} -\nabla \mathcal{L}(\mathbf{x}_i, \lambda_i) \\ c(\mathbf{x}_i) \end{bmatrix} \quad (23)$$

for some \mathbf{p}_i and μ_i . The updated estimates of \mathbf{x}^* and λ^* are therefore calculated by

$$\mathbf{x}_{i+1} = \mathbf{x}_i + \alpha_i \mathbf{p}_i \quad (24)$$

$$\lambda_{i+1} = \lambda_i + \alpha_i \mu_i \quad (25)$$

where $\alpha_i \in (0, 1]$ is an adjustable step-size parameter chosen to satisfy the so-called Wolfe conditions [31], [32]. The algorithm is iterative and terminates when the step change is less than a pre-determined tolerance $\gamma \geq 0$ such that $\|\mathbf{x}_{i+1} - \mathbf{x}_i\| \leq \gamma$.

A logical choice (assuming zero-mean errors) for the initial error estimates is $\mathbf{e} = \mathbf{0}$ where $\mathbf{e} = [e_1, e_2, e_3, \dots]$ or $\mathbf{e} = [e_{\theta 1i}, e_{\phi 1i}, e_{\theta i1}, e_{\phi i1}, \dots]$ is the error vector. The initialization is geometry-invariant and the initial estimate

corresponds to a meaningful statistic of the parameter being estimated since in the majority of cases the mean error values are assumed known. Hence, our algorithm provides a non-trivial and practically important advantage over the traditional formulated maximum likelihood algorithm. Since the TML techniques optimize directly against the target location, they often require an initial estimate of this position. A meaningful and accurate statistic of the true target location is much more difficult to obtain when compared to the statistics of the measurement errors.

Following the convergence of the optimization algorithm we have an estimate of the measurement error vector \mathbf{e} . According to the constraints ((2), (7) or (12)) and ((1) or (12)), it is this error value *subtracted* from the corresponding *measured* angle value that results in equation consistency along with estimates of the true angle values. Therefore, we subtract the appropriate error from the appropriate *measured* angle (e.g. in (1) or (12)) and localize the target with any closed-form triangulation method. It is possible to solve any well-determined subset of the overdetermined equation system for the unique location solution.

Remark 4: When the measurement errors are assumed small it may be possible to replace the nonlinear constraints given in Theorems 1, 2 and 3 by their small angle approximated counterparts. That is, we can employ the following trigonometric approximations; $\sin(e_i) \approx e_i$ and $\cos(e_i) \approx 1$ etc. When the angles are given in radians, the approximation $\sin(e_i) \approx e_i$ exhibits an approximate error of 1% at about $\pi/12$ radians (or 15°). Furthermore, in such a case the multiplication $e_i e_j$ can be approximated as $e_i e_j \approx 0$ (again for $e_i = e_j < \pi/12$ radians (or 15°) we have $e_i e_j < 0.0685$). Noting that $\pi/12$ radians (or 15°) is a rather large error, this approximation may be acceptable in some applications. Following the same reasoning it is possible to approximate any higher order term (e.g. $e_i e_j e_k$) by 0. The result is an affine linear constraint and a simple optimization problem (e.g. least squares) that can be solved analytically very easily. Thus, we have a closed-form analytical alternative to the numerical SQP algorithm for small error environments and good localization geometries.

We employ the Matlab Optimization Toolbox (2006, v3) function *fmincon* to implement the SQP technique. Although the specific details may vary from one implementation of SQP to another, in our case the specific implementation should not greatly effect the optimization performance.

V. NUMERICAL SIMULATION

In order to illustrate the proposed localization algorithm we perform a number of illustrative examples. The goal of these simulations is to illustrate the superior performance of our GCLS algorithm in geometries traditionally adverse to accurate localization performance. We compare the geometrically constrained optimization algorithm developed in this paper (denoted GCLS) against the traditional maximum likelihood algorithm (denoted TML) and against the simple closed-form mean location calculation (denoted MEAN). The GCLS algorithm is initialized with $e_i = 0$ while the TML algorithm is initialized with the closed-form mean location estimate. The

numerical (iterative) algorithms are said to diverge when the RMS position errors go above $\pm 10^6$.

A. Examples in \mathbb{R}^2

The errors in the azimuth bearing measurements obey a zero-mean Gaussian distribution with standard deviation denoted by σ_θ .

1) *Non-Collinear Sensors:* We examine the performance of the constraint given in Theorem 1 first. We consider three sensors and a single target. We explore the localization techniques discussed in a geometric environment well-suited to accurate localization. We consider the scenario given in Figure 4 (a).

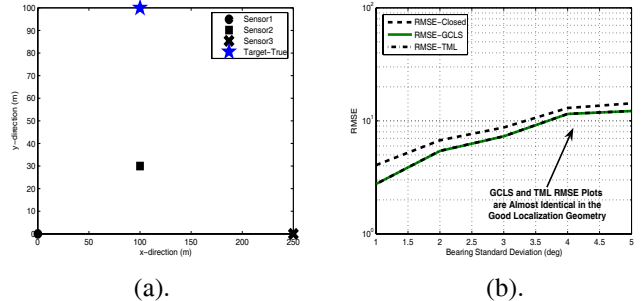


Fig. 4. In (a), the good localization geometry is illustrated. In (b), the RMSE over 1000 simulation runs is given.

In Figure 4 (b) we plot the RMS position errors for the GCLS, TML and MEAN estimates for a bearing standard deviation ranging from $\sigma_\theta = 1^\circ$ to $\sigma_\theta = 5^\circ$ and over 1000 simulation runs. In the good localization geometry depicted in Figure 4 (a) we observe the GCLS and TML algorithms outperform the MEAN estimate as expected. Moreover, we notice that the TML and GCLS algorithms perform almost exactly the same. This is because both algorithms are essentially different parameterizations of the maximum likelihood technique. However, we will subsequently show that in adverse localization geometries our algorithm will significantly outperform the TML algorithm which requires an initial estimate that is geometry-dependent while our GCLS algorithm's initialization is geometry-invariant and can be related to known error statistics such as the error mean values.

Therefore, we now consider the scenario depicted in Figure 5 (a) where the target location relative to the sensor positions is clearly adverse to accurate localization. In this simulation we expect the TML algorithm to diverge in at least a number of simulation runs due to poor initialization.

In Figure 5 (b) we plot the RMS position errors for the GCLS and MEAN estimates for a bearing standard deviation ranging from $\sigma_\theta = 1^\circ$ to $\sigma_\theta = 5^\circ$ and over 1000 simulation runs. From Figure 5 (b) we notice that the GCLS algorithm significantly outperforms the MEAN estimate as expected. The TML algorithm is not plotted in Figure 5 (b) since it diverges in too many simulation runs as indicated in Table I while the GCLS algorithm diverged in none.

When the TML algorithm did converge its performance was comparable with the GCLS algorithm as shown in the previous

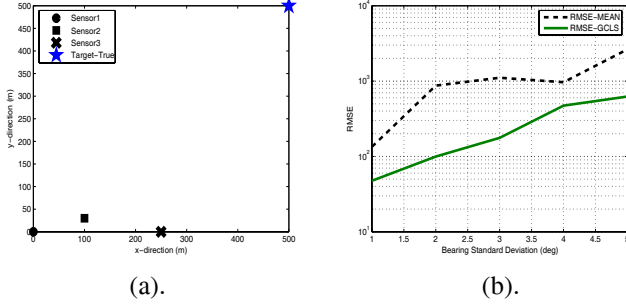


Fig. 5. In (a), the adverse localization geometry is illustrated. In (b), the RMSE over 1000 simulation runs is given.

TABLE I

DIVERGENCE OF THE TML ALGORITHM IN \mathbb{R}^2 WITH BAD GEOMETRY

Standard Deviation σ_θ	1°	2°	3°	4°	5°
Approx. Divergence %	2	10	10	10	15

simulation example. It is well known that the initialization of nonlinear least squares algorithms is a significant factor in convergence of numerical algorithms. However, we have shown that our algorithm can be initialized in a geometry independent fashion using known (or assumed known) error statistics. We believe these simulations illustrate that this by no means a trivial advantage over traditional maximum likelihood localization techniques which cannot easily be initialized with an accurate statistic. Since the TML algorithm is initialized with the closed-form MEAN estimate it is also reasonable to conclude that as the measurement noise increases or the geometry becomes more adverse and hence the MEAN estimate performs worse, then it will be even more difficult to initialize the TML algorithm.

2) *Multiple Sensors and Constraints*: Now we will turn our attention to the case involving multiple constraints. Let us assume that we have three collinear sensors and a fourth sensor that is not collinear with any multiple combination of the other sensors. Hence, we can derive two independent constraints of the form

$$\begin{aligned} c_1(e_1, e_2, e_3) &= 0 \\ c_2(e_1, e_2, e_4) &= 0 \end{aligned}$$

where the form of the constraints may both be as (10) or the one for the three collinear sensors may be as (2). Since the constraints of the form (10) account for all geometric configurations we will consider both constraints to be of this form. In good localization geometries it can be shown, as expected, that the TML algorithm performs comparably with the GCLS algorithm and both optimization approaches outperform the MEAN estimate. Thus, for brevity, we will only consider geometries adversely suited to accurate localization. The scenario is depicted in Figure 6 (a) where the target location relative to the sensor positions is clearly adverse to accurate localization. Moreover, the long target range illustrated means the target appears almost collinear with the sensors depicted in Figure 6 (a).

In Figure 6 (b) we plot the RMS position errors for the GCLS and MEAN estimates for a bearing standard deviation

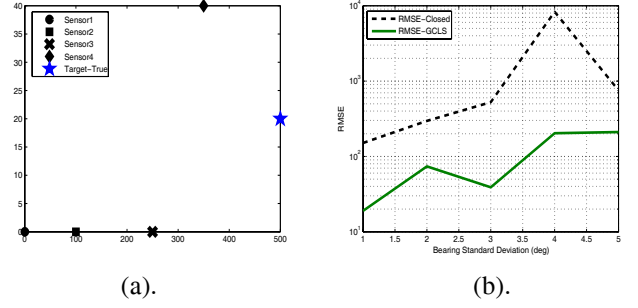


Fig. 6. In (a), the adverse localization geometry is illustrated. In (b), the RMSE over 1000 simulation runs is given.

ranging from $\sigma_\theta = 1^\circ$ to $\sigma_\theta = 5^\circ$ and over 1000 simulation runs. From Figure 6 (b) we notice that the GCLS algorithm significantly outperforms the MEAN estimate as expected. The TML algorithm is not plotted in Figure 6 (b) since it diverges in too many simulation runs as indicated in Table II while the GCLS algorithm diverged in none.

TABLE II

DIVERGENCE OF THE TML ALGORITHM IN \mathbb{R}^2 WITH MULTIPLE CONSTRAINTS AND BAD GEOMETRY

Standard Deviation σ_θ	1°	2°	3°	4°	5°
Approx. Divergence %	5	15	15	20	20

When the TML algorithm did converge it's performance was comparable with the GCLS algorithm as shown in the previous simulation examples. Again we have shown that our algorithm can be initialized in a geometry independent fashion using known (or assumed known) error statistics and we believe these simulations illustrate that this by no means a trivial advantage over traditional maximum likelihood localization techniques.

B. Examples in \mathbb{R}^3

Similarly to the \mathbb{R}^2 problem we will now examine the localization problem in \mathbb{R}^3 . The errors in the bearing measurements obey a zero-mean Gaussian distribution with standard deviation denoted by $\sigma_\theta = \sigma_\phi$.

In \mathbb{R}^3 it can again be shown that in good localization geometries that the TML algorithm performs comparably with the GCLS algorithm and both optimization approaches outperform the MEAN estimate. Thus, for brevity, we will only consider geometries in \mathbb{R}^3 adversely suited to accurate localization. The scenario is depicted in Figure 7 (a) where the target location relative to the sensor positions is clearly adverse to accurate localization.

In Figure 7 (b) we plot the RMS position errors for the GCLS and MEAN estimates for a bearing standard deviation ranging from $\sigma_\theta = \sigma_\phi = 1^\circ$ to $\sigma_\theta = \sigma_\phi = 5^\circ$ and over 1000 simulation runs. From Figure 7 (b) we notice that the GCLS algorithm significantly outperforms the MEAN estimate as expected. The TML algorithm is not plotted in Figure 7 (b) since it diverges in too many simulation runs as indicated in Table III while the GCLS algorithm diverged in none.

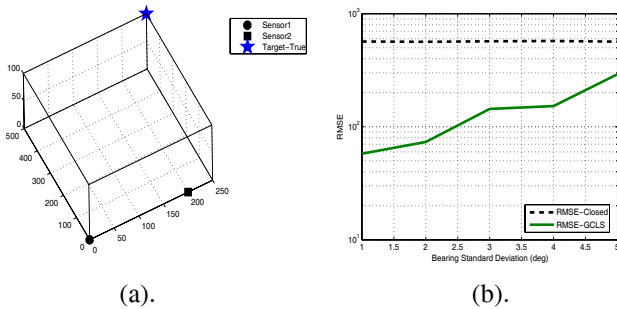


Fig. 7. In (a), the adverse localization geometry is illustrated. In (b), the RMSE over 1000 simulation runs is given.

TABLE III

DIVERGENCE OF THE TML ALGORITHM IN \mathbb{R}^3 WITH BAD GEOMETRY

Standard Deviation $\sigma_\theta = \sigma_\phi$	1°	2°	3°	4°	5°
Approx. Divergence %	95	95	95	95	95

From Table III we note that the TML algorithm diverges in practically every simulation run for the adverse geometric localization problem depicted in Figure 7 (a). When the TML algorithm did converge it's performance was comparable with the GCLS algorithm as shown in the previous simulation examples. Again we have shown that our algorithm can be initialized in a geometry independent fashion using known (or assumed known) error statistics and we believe these simulations illustrate that this by no means a trivial advantage over traditional maximum likelihood localization techniques. Similar results in \mathbb{R}^3 can also be shown with multiple sensors and constraints.

C. General Discussion

From our simulations we note that the constrained optimization estimate outperforms the other approaches illustrated in particular in adverse localization geometries. The traditional maximum likelihood (TML) approach unfortunately suffers from initialization problems and in general is not practically suited to localization in such geometries, albeit the underlying goal of TML is to find an optimal location solution. Our GCLS algorithm addresses the practical problems inherent in the TML algorithm by removing the effect of the geometry on the initialization routines. That is, our GCLS algorithm initialization is geometry-invariant and only depends on the expected values of the measurement errors. Hence, our algorithm is both theoretically and practically justified to perform optimally in such geometries. In \mathbb{R}^3 we can particularly see the advantage of the geometrically constrained localization algorithm over both the simple closed-form approach and over the traditionally formulated maximum likelihood algorithm.

Finally we have remarked previously that although we employ a least squares objective function, we are by no means restricted to doing so. Our geometric constraint is invariant to the cost function associated with the optimization problem. Therefore, if it turns out that some other objective is better suited to a given problem then it is a simple matter to adapt our approach appropriately.

VI. CONCLUSION

This paper introduced a constraint on the errors in bearing-measurement based localization systems. The constraint we have derived accounts for the underlying geometry, measurements and the nature of the true bearing errors and it is invariant to the cost function. The localization problem is formulated as a constrained optimization problem and the resulting location estimate outperforms the traditional least squares (maximum likelihood) approach in a number of respects. In particular, the iterative algorithm developed in this paper can be easily initialized with a meaning error statistic that is often known. The traditionally formulated maximum likelihood approach has been well-known to suffer from initialization problems leading to divergence.

REFERENCES

- [1] R.O. Schmidt. Multiple emitter location and signal parameter estimation. *IEEE Transactions on Antennas and Propagation*, AP-34(3):276–280, March 1986.
- [2] R. Roy and T. Kailath. Esprit - estimation of signal parameters via rotational invariance techniques. *IEEE Transactions on Acoustics, Speech, and Signal Processing*, 37(7):984–995, July 1989.
- [3] P. Stoica and K.C. Sharman. Maximum likelihood methods for direction of arrival estimation. *IEEE Transactions on Acoustics, Speech, and Signal Processing*, 38(7):1132–1143, July 1990.
- [4] A.J. Barabell. Improving the resolution performance of eigenstructure-based direction-finding algorithms. In *Proc. ICASSP*, pages 336–339, Boston, MA, 1983.
- [5] R.G. Stansfield. Statistical theory of D.F. fixing. *Journal Institution Electrical Engineering*, 94(15):186–207, 1947.
- [6] H.E. Daniels. The theory of position finding. *Journal of the Royal Statistical Society*, B13:186–207, 1951.
- [7] M. d'Ocagne. Sur la determination geometrique du point le plus probable donne par un systeme de droites non convergentes. *Journal de l'Ecole Polytechnique*, (63):1–25, 1893.
- [8] M. Gavish and A.J. Weiss. Performance analysis of bearing-only target location algorithms. *IEEE Transactions on Aerospace and Electronic Systems*, 28(3):817–827, 1992.
- [9] D.J. Torrieri. Statistical theory of passive location systems. *IEEE Transactions on Aerospace and Electronic Systems*, 20(2):183–198, March 1984.
- [10] W.H. Foy. Position-location solutions by Taylor-series estimation. *IEEE Transactions on Aerospace and Electronic Systems*, 12(2):187–194, March 1976.
- [11] S.C. Nardone, A.G. Lindgren, and K.F. Gong. Fundamental properties and performance of conventional bearings-only target motion analysis. *IEEE Transactions on Automatic Control*, AC-29(9):775–787, 1984.
- [12] K.R. Pattipati, D. Somnath, Y. Bar-Shalom, and R.B. Washburn Jr. A new relaxation algorithm and passive sensor data association. *IEEE Transactions on Automatic Control*, 37(2):198–213, February 1992.
- [13] S. Deb, M. Yeddanapudi, K.R. Pattipati, and Y. Bar-Shalom. A generalized S-D assignment algorithm for multisensor-multitarget state estimation. *IEEE Transactions on Aerospace and Electronic Systems*, 33(2), April 1992.
- [14] R.L. Popp, K.R. Pattipati, and Y. Bar-Shalom. m-Best S-D assignment algorithm with application to multitarget tracking. *IEEE Transactions on Aerospace and Electronic Systems*, 37(1), January 2001.
- [15] H.W.L. Naus and C.V. Wijk van. Simultaneous localisation of multiple emitters. *IEE Proc. on Radar, Sonar, and Navigation*, 151(2), April 2004.
- [16] A.N. Bishop and P.N. Pathirana. A discussion on passive location discovery in emitter networks using angle-only measurements. In *Proceedings of the 2006 International Wireless Communications and Mobile Computing Conference*, pages 1337–1343, Vancouver, British Columbia, Canada, 2006.
- [17] A.N. Bishop and P.N. Pathirana. Localization of emitters via the intersection of bearing lines: A ghost elimination approach. *IEEE Transactions on Vehicular Technology*, To Appear 2007.
- [18] A.G. Lindgren and K.F. Gong. Position and velocity estimation via bearing observations. *IEEE Transactions on Aerospace and Electronic Systems*, 14(4):564–577, July 1978.

- [19] E. Fogel and M. Gavish. n^{th} -order dynamics target observability from angle measurements. *IEEE Transactions on Aerospace and Electronic Systems*, 24(3), 1988.
- [20] S.C. Nardone and M.L. Graham. A closed-form solution to bearings-only target motion analysis. *IEEE Transactions on Oceanic Engineering*, 22(1):168–178, January 1997.
- [21] K. Dogancay. Bias compensation for the bearings-only pseudolinear target track estimator. *IEEE Transactions on Signal Processing*, 54(1):59–68, January 2006.
- [22] R.I. Hartley and P. Sturm. Triangulation. *Computer Vision and Image Understanding*, 68(2):146–157, November 1997.
- [23] R. I. Hartley and A. Zisserman. *Multiple View Geometry in Computer Vision*. Cambridge University Press, 2nd edition, 2004.
- [24] H. Stewenius, F. Schaffalitzky, and D. Nister. How hard is 3-view triangulation really? In *Tenth IEEE International Conference on Computer Vision (ICCV)*, pages 686–693, October 2005.
- [25] M. Cao, B.D.O. Anderson, and A.S. Morse. Localization with imprecise distance information in sensor networks. *Systems and Control Letters*, 55(11):887–893, November 2006.
- [26] R.S. Engelbrecht. Passive source localization from spatially correlated angle-of-arrival data. *IEEE Transactions on Acoustics, Speech, and Signal Processing*, 31(4):842–846, August 1983.
- [27] K. Dogancay and G. Ibal. Instrumental variable estimator for 3D bearings-only emitter localization. In *ISSNIP*, pages 63–68, Melbourne, Australia, 2005.
- [28] R. Fletcher. *Practical Methods of Optimization: Vol 2: Constrained Optimization*. John Wiley and Sons, 1981.
- [29] D.P. Bertsekas. *Constrained Optimization and Lagrange Multiplier Methods*. Athena Scientific, 1996.
- [30] P.E. Gill, W. Murray, and M.H. Wright. *Practical Optimization*. Academic Press, 1981.
- [31] P. Wolfe. Convergence conditions for ascent methods. *SIAM Review*, 11(2):226–235, April 1969.
- [32] P. Wolfe. Convergence conditions for ascent methods, II: Some corrections. *SIAM Review*, 13(2):185–188, April 1971.